The EMBO Journal Vol.16 No.9 pp.2493–2506, 1997

Histone octamer function *in vivo*: mutations in the dimer–tetramer interfaces disrupt both gene activation and repression

Maria Soledad Santisteban, Gina Arents[1], Evangelos N.Moudrianakis[1] and M.Mitchell Smith[2]

Department of Microbiology and University of Virginia Cancer Center, Box 441 Jordan Building, School of Medicine, University of Virginia, Charlottesville, VA 22908 and [1]Department of Biology, The Johns Hopkins University, Baltimore, MD 21218, USA

[2]Corresponding author
e-mail: mms7r@Virginia.EDU

Within the core histone octamer each histone H4 interacts with each H2A–H2B dimer subunit through two binding surfaces. Tyrosines play a central role in these interactions with H4 tyrosines 72 and 88 contacting one H2A–H2B dimer subunit, and tyrosine 98 contacting the other. To investigate the roles of these interactions *in vivo*, we made site-directed amino acid substitutions at each of these tyrosine residues. Elimination of either set of interactions is lethal, suggesting that binding of the tetramer to both dimers is essential. Temperature-sensitive mutants were obtained through single amino acid substitutions at each of the tyrosines. The mutants show both strong positive and negative effects on transcription. Positive effects include Spt- and Sin-phenotypes resulting from mutations at each of the three tyrosines. One allele has a strong negative effect on the expression of genes essential for the G_1 cell cycle transition. At restrictive temperature, mutant cells fail to express the *CLN1*, *CLN2*, *SWI4* and *SWI6* genes, and have reduced levels of *CLN3* mRNA. These results demonstrate the critical role of histone dimer–tetramer interactions *in vivo*, and define their essential role in the expression of genes regulating G_1 cell cycle progression.

Keywords: cell division cycle/chromatin/nucleosome structure/*Saccharomyces cerevisiae*

Introduction

The fundamental unit of chromatin organization, the histone core complex, is maintained as an octamer by two types of protein–protein interactions (Eickbush and Moudrianakis, 1978). One class is the strong interaction between H3 and H4 within the tetramer, and between H2A and H2B within the dimer subunits. The second class is the weaker interaction between the $[H3–H4]_2$ tetramer and the two [H2A–H2B] dimer subunits. These dimer–tetramer interactions are of considerable interest because they are proposed to play important roles in many aspects of chromosome function.

DNA replication is one such candidate function. Chromatin assembly *in vivo* is thought to occur through the stepwise deposition of histone subunits onto newly replicated DNA. Biochemical experiments have shown that $[H3–H4]_2$ tetramers are deposited first during assembly, and then nucleosome formation is completed with the later addition of [H2A–H2B] dimers (Worcel *et al*., 1978; Smith *et al.*, 1984). Several *in vitro* studies with replication-coupled chromatin assembly systems are consistent with this two-step model (Dilworth *et al*., 1987; Almouzni *et al.*, 1990). It has also been suggested that pre-existing histone octamers may dissociate into tetramers and dimers during replication (Jackson, 1990). Thus, these interactions could be significant both for the assembly of new nucleosomes, and for the rearrangement of old nucleosomes during replication.

Several lines of evidence suggest that RNA transcription is also likely to depend on functional histone dimer–tetramer interactions. *In vivo*, histone [H2A–H2B] dimers are in dynamic exchange in the chromatin, part of which appears to depend on RNA polymerase activity (Jackson, 1990). Biochemical and physical analyses of nucleosomes from chromatin partially enriched for actively transcribing genes have indicated an altered structure consistent with the depletion of one of the [H2A–H2B] dimers (Baer and Rhodes, 1983; Locklear *et al.*, 1990). Strong support for a role for dimer–tetramer interactions in transcription is also provided by genetic experiments in *Saccharomyces cerevisiae* where normal transcription depends on the balanced gene dosage of the histone gene sets. Changes in the normal ratio of the histone H2A–H2B gene sets relative to the H3–H4 gene sets, either too high or too low, can alter the selection of specific gene promoters (Clark-Adams *et al*., 1988) and bypass the need for positive transcriptional activation complexes, presumably by disrupting normal chromatin architecture (Hirschhorn *et al*., 1992). Recently, bypass mutants in transcriptional activation were identified in histones H3 and H4, and one class of such mutants were in the histone fold facing the [H2A–H2B] interface of the octamer (Kruger *et al.*, 1995). A variety of studies *in vitro* are consistent with these results. For example, nucleosomes lacking one [H2A–H2B] dimer interact with RNA polymerase more strongly than the complete nucleosome core (Gonzalez *et al.*, 1987) and are transcribed more efficiently (Gonzalez and Palacian, 1989). In addition, the histone-binding protein nucleoplasmin facilitates the binding of the transcription factors GAL4-AH, USF and SP1 to nucleosomal DNA through the sequential displacement of [H2A–H2B] dimers followed by H3–H4 tetramer displacement onto competing DNA (Chen *et al.*, 1994).

The role of dimer–tetramer interactions in transcription may not be confined to single nucleosomes. It has been proposed that depletion of [H2A–H2B] dimers may disrupt the ability of nucleosome arrays to fold into higher-order structures, and thereby relieve transcriptional repression (Hansen and Wolffe, 1994). Consistent with this hypo-

thesis, changes in the dosage of the H2A–H2B gene sets in *S.cerevisiae* have been reported to alter the chromatin over certain chromosomal regions (Norris *et al.*, 1988).

Finally the altered stoichiometry of the core histones produced by imbalanced expression of the octamer subunits also impairs the fidelity of mitotic chromosome transmission, suggesting possible roles for these dimer–tetramer interactions in chromosome behavior during mitosis (Meeks-Wagner and Hartwell, 1986; Smith and Stirling, 1988).

All of these results suggest that interactions between dimer and tetramer subunits of the protein core of the nucleosome may be critical for normal nuclear functions. Here we report the results of the first direct genetic analysis of these interactions and their roles in gene expression. Based on the X-ray crystal model of the histone octamer, we perturbed the dimer–tetramer interface with site-directed mutations and examined the effects of these mutations on transcription, cell cycle progression and general viability in the budding yeast *S.cerevisiae*. The phenotypes of these mutants show that disruption of the normal dimer–tetramer interactions can have both strong positive and negative effects on gene transcription, and define a new role for chromatin structure in the regulation of G_1 progression in the cell division cycle.

Results

Selection of tyrosines for mutagenesis

In choosing sites for directed mutations that would specifically alter the dimer–tetramer interfaces of the histone octamer, we focused on tyrosine residues in H4 based on the results of both solution and crystallographic studies. Early findings from solution physicochemical studies (Eickbush and Moudrianakis, 1978) demonstrated that the core histone octamer in solution behaves as a tripartite thermodynamic entity in reversible equilibrium with its subunits, one $[H3–H4]_2$ tetramer and two [H2A–H2B] dimers. Analysis of the properties of this equilibrium led directly to the proposal that the centrally located tetramer interacts with the two flanking dimers via a limited number of contacts that include essential tyrosines. The reversible modulation of these interfacial contacts was proposed to be responsible for the functional cycles of chromatin. The importance of tyrosine contacts for histone octamer structure has since been supported by a wide variety of biophysical studies involving both spectroscopic analysis (Butler and Olins, 1982; Michalski-Scrive *et al.*, 1982) and chemical modifications (Chan and Piette, 1982; Kleinschmidt and Martinson, 1984; Zweidler, 1992).

The tripartite organization of the histone octamer and the involvement of tyrosines in the integrity of the structure were confirmed by crystallographic studies (Arents *et al.*, 1991; Arents and Moudrianakis, 1993) that also identified a common architectural motif among the four core histones, termed the histone fold (Arents and Moudrianakis, 1993). The core octamer of the nucleosome contains four structural subunits, in three thermodynamic domains, creating a left-hand superhelical protein ramp (Arents *et al.*, 1991). Proceeding into the octamer structure along the superhelical axis, the order of dimer subunits is $[H2A^1–H2B^1]$, $[H3^1–H4^1]$, $[H3^2–H4^2]$ and $[H2A^2–H2B^2]$. Figure 1A shows a view of the histone octamer, looking down the superhelical axis, with the molecular 2-fold axis horizontal. In this view, the $[H2A^2–H2B^2]$ dimer subunit (blue) and the $[H3^2–H4^2]$ dimer subunit (H3 green and H4 white) comprise most of the visible structure, with a portion of $H3^1$ (green) also visible in the lower left quarter of the structure.

The interfaces between the centrally located tetramer and the flanking dimers are formed from both fold and non-fold elements and contain a number of tyrosine residues in two distinct groupings. In the first group, tyrosine 72 (Y72) and tyrosine 88 (Y88) of H4 interact with one of the flanking [H2A–H2B] dimers, while tyrosine 98 (Y98) interacts with the other. This is illustrated in Figure 1B where the $[H2A^2–H2B^2]$ dimer has been removed, exposing Y98 (black) of $H4^1$ which interacts with that dimer. On the other hand, Y72 (yellow) and Y88 (red) of $H4^1$ are only partially visible because they are in contact with the remaining $[H2A^1–H2B^1]$ dimer in the figure. The back view shown in Figure 1C reveals the interactions of the other $H4^2$ subunit. In this view, it can be seen that removal of the $[H2A^2–\ H2B^2]$ dimer has exposed Y72 (yellow) and Y88 (red) of $H4^2$ where they would normally make contact with that dimer. The Y98 residue of $H4^2$ is not visible in this view because it is in contact with the remaining $[H2A^1–H2B^1]$ dimer and covered by that dimer. The symmetry of these interactions is illustrated in Figure 1D in which just the $[H3–H4]_2$ tetramer is shown. Thus, one of the major features of the dimer–tetramer interactions in the histone octamer is that each of the H4 molecules in the $[H3–H4]_2$ tetramer touches both [H2A–H2B] dimer subunits across the dimer–tetramer interfaces.

Further details of these interactions are depicted in the ribbon representation shown in Figure 1E. In this view of the octamer, the $[H3^1–H4^1]$ dimer subunit has been removed from the model for clarity, leaving the dimers $[H2A^1–H2B^1]$, $[H3^2–H4^2]$ and $[H2A^2–H2B^2]$. The two groupings of interactions described above are apparent. In the first group, where $[H2A^2–H2B^2]$ contacts the tetramer, the histone fold part of H4 interacts with the histone fold part of H2B to form a four-helix bundle. Although a number of residues from both H2B and H4 contribute to this interface, one of the most striking features of the interface is the large hydrophobic domain generated by the contacts between three tyrosines: Y72 and Y88 from H4, and Y83 from H2B. These three tryrosines form a cluster in which the planes of the side chains are approximately perpendicular to each other. In the second group, the contact between $H4^2$ and $[H2A^1–H2B^1]$ arises from a non-fold, extended chain arm of H4 running roughly parallel to a non-fold, extended chain arm of H2A. Most of these contacts arise from main chain interactions. Within this interface, however, Y98 of $H4^2$ is exceptional due to the insertion of the large tyrosyl ring into a cleft in the dimer surface. Symmetrical interactions occur with the other $[H3^1–H4^1]$ dimer subunit not shown in this representation. Thus, there are two distinct classes of interactions between histone H4 and the [H2A–H2B] dimers, and both biophysical and structural studies have identified tyrosine residues as key participants in each type of interaction.

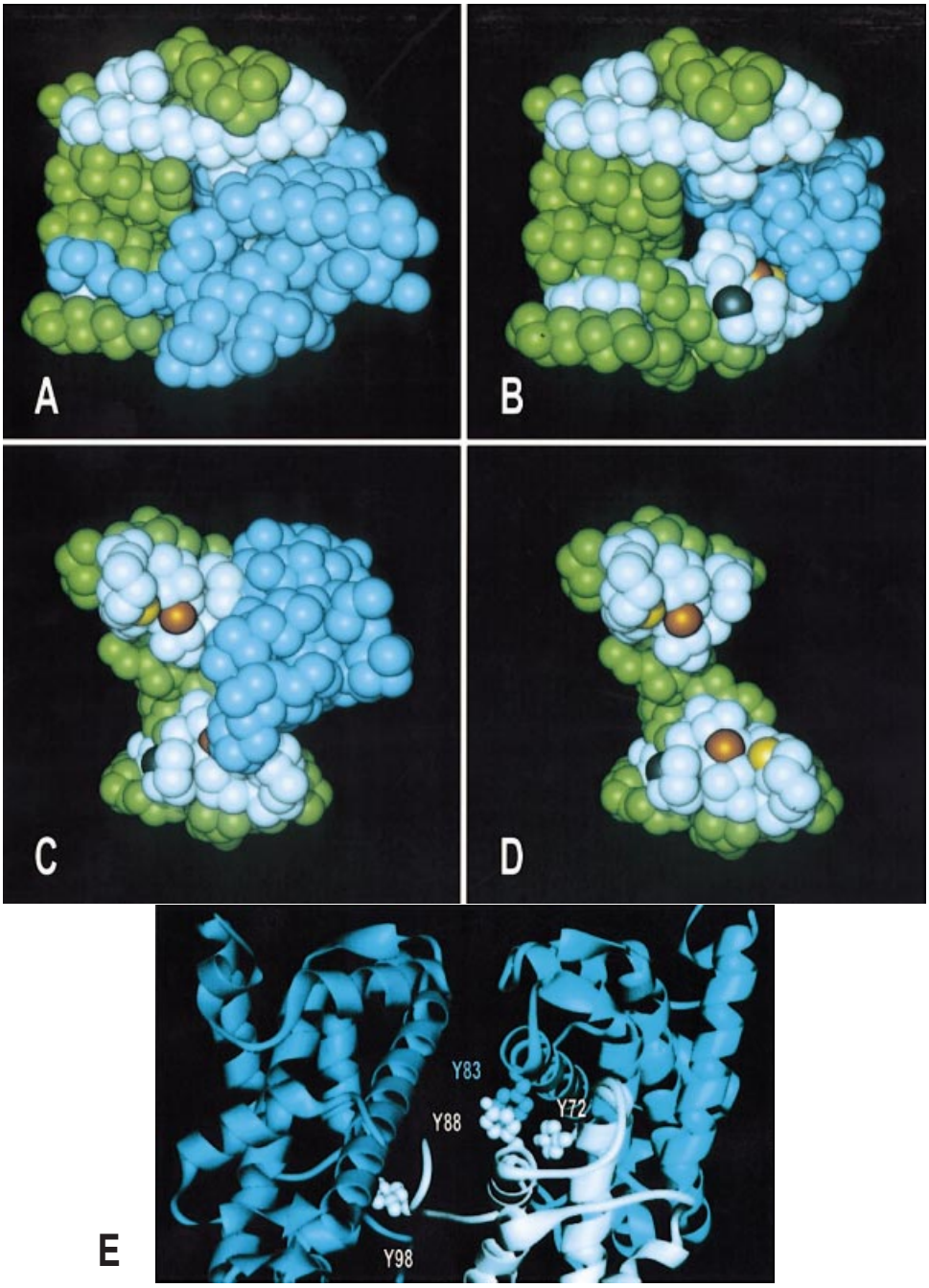

Fig. 1. Tyrosine residues in the dimer–tetramer interfaces of the core histone octamer. (**A**) View of the histone octamer looking down the superhelical axis with the molecular 2-fold axis horizontal from left to right. (**B**) Same view as (A), but with the second dimer subunit, [$H2A^2$–$H2B^2$], removed to expose the buried interface. (**C**) A view of the hexamer substructure model shown in (B), created by rotating 90° around the vertical axis, looking down the molecular 2-fold axis from the 'back'. (**D**) Same view as (C) with the other dimer subunit, [$H2A^1$–$H2B^1$], also removed leaving just the $[H3–H4]_2$ tetramer. For (A–D), histone H4 is white, histone H3 is green and the H2A–H2B dimer subunits are blue. Histone H4 Tyr72 is yellow, Tyr88 is red and Tyr98 is black. (**E**) A ribbon representation illustrating the relationship of the two [H2A–H2B] dimer subunits with the [$H3^2$–$H4^2$] dimer subunit. In this view, the molecular 2-fold axis is vertical, running from bottom to top. The [$H3^1$–$H4^1$] dimer subunit has been removed from this picture for clarity. Interactions symmetrical with those shown for the [$H3^2$–$H4^2$] dimer subunit in the panel are formed by the [$H3^1$–$H4^1$] dimer subunit as well. The [$H2A^1$–$H2B^1$] dimer is dark blue, the [$H3^2$–$H4^2$] dimer is white and the [$H2A^2$–$H2B^2$] dimer is light blue. The H4 tyrosines Y72, Y88 and Y98 (white) and the H2B tyrosine Y83 (blue) are modeled with the tyrosyl ring shown.

Construction and properties of mutants

Based on these structural considerations, we constructed mutant histone H4 alleles with amino acid substitutions at positions 72, 88 and 98. In the initial series of constructs, the tyrosine codons at these positions were changed to glycine codons, creating mutant alleles *hhf1-36* (Y72G), *hhf1-37* (Y88G) and *hhf1-38* (Y98G). The wild-type gene and each of these new mutant alleles were integrated at the *LEU2* locus on chromosome III, providing the only source of histone H4 in their respective cells (see Materials and methods). These ectopic integrations produced a set of strains that were isogenic except for their histone H4 alleles.

As can be seen in Figure 2, all three mutants have

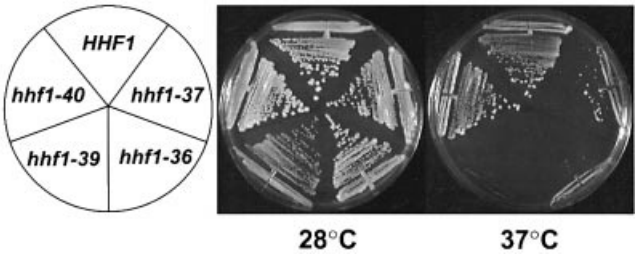

Fig. 2. Conditional growth of histone H4 tyrosine mutants. Growth is shown on YPD plates for wild-type and four histone H4 mutant strains after incubation for 5 days at 28 or 37°C. All the strains were isogenic except for the histone H4 alleles: WT (*HHT1*), Y98W (*hhf1-40*), Y98H (*hhf1-39*), Y88G (*hhf1-37*) and Y72G (*hhf1-36*).

detectable growth phenotypes. Both *hhf1-36* (Y72G) and *hhf1-37* (Y88G) cells grow somewhat more slowly than the control *HHF1* strain at 28°C, and are temperature sensitive (Ts^-) for growth at 37°C. Of the two, *hhf1-36* is the more severe allele. The third allele, *hhf1-38* (Y98G), is lethal. Cells with *hhf1-38* integrated at the *LEU2* locus could be propagated only in the presence of plasmid pMS329, a single copy *URA3* plasmid that expresses the wild-type *HHF1* histone H4 gene. When this strain was transferred to medium contain 5-fluoroorotic acid (5-FOA) to select for cells that had lost the *URA3* pMS329 plasmid, it failed to give colonies, indicating that *hhf1-38* alone does not support cell growth. This result is consistent with previous deletion studies in which an H4 mutant with a carboxy-terminal truncation of residues 100–102 was found to be viable, whereas a truncation of residues 97–102 was dead (Kayne *et al.*, 1988). Together, these results suggest an essential role for Y98 in H4 function.

We next constructed additional alleles with point mutants at position 98 by making more conservative changes, replacing tyrosine with either histidine (*hhf1-39*, Y98H) or tryptophan (*hhf1-40*, Y98W). Figure 2 shows that *hhf1-40* (Y98W) cells grow normally at both 28 and 37°C. In fact, *hhf1-40* mutants are wild-type for all phenotypes tested to date. In contrast, *hhf1-39* grows poorly at 28°C, and is Ts^- lethal at 37°C (Figure 2). Thus, the function of histone H4 is highly sensitive to substitutions at position 98: tyrosine or tryptophan support wild-type function, histidine is only partially functional and glycine is lethal.

The phenotypic pattern of the single substitution mutants paralleled the structural interactions of H4 with the [H2A–H2B] dimer subunits. Tyr98 is the sole site of tyrosine interaction with one of the [H2A–H2B] dimers in the core octamer, whereas Y72 and Y88 both interact simultaneously with the other. Based on this model, we predicted that the Y72G,Y88G double mutant might be lethal by completely disrupting the tyrosine interactions with the second [H2A–H2B] dimer. In order to test this hypothesis, we constructed the double substitution allele, *hhf1-41*. Strains with *hhf1-41* integrated at the *LEU2* locus could be grown only in the presence of pMS329 carrying the wild-type *HHF1* gene, and loss of pMS329 resulted in cell death. Thus, this double substitution allele is lethal as predicted.

Chromatin structure of H4 tyrosine mutants

The overall chromatin structure of the viable H4 tyrosine mutants was examined by micrococcal nuclease digestions.

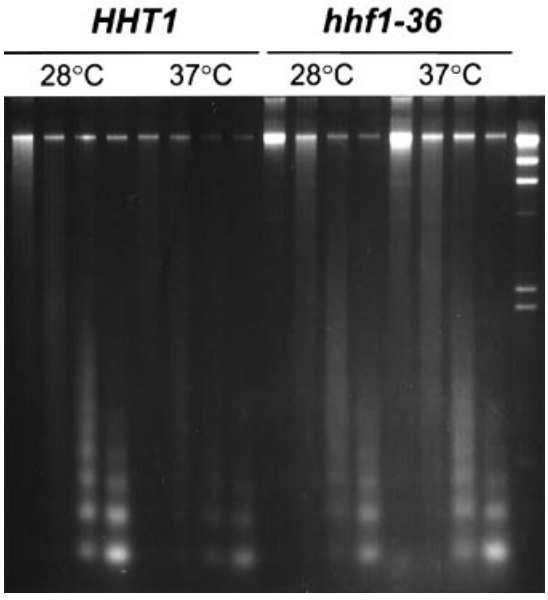

Fig. 3. Micrococcal nuclease digestion of chromatin. The ethidium bromide staining of the nuclease-digested chromatin is shown for wild-type (*HHT1*) and Y72G (*hhf1-36*) mutant strains, both for cells grown at 28°C and after 3 h at 37°C. Similar nucleosome ladders can be observed for the mutant, the wild-type strain and the mutant at 37°C.

The result for *hhf1-36*, which has the most severe phenotype, is shown in Figure 3. At both permissive and restrictive temperatures no differences were detected in the oligonucleosome ladders produced by partial micrococcal nuclease digestion. Similar results were obtained for *hhf1-37* and *hhf1-38* (data not shown). These results indicate that there is no gross defect in the general organization of nucleosomes in the H4 tyrosine mutants at either the permissive or restrictive temperature, and are similar to those obtained for the overall chromatin structure of histone H2A and H2B gene dosage mutants (Norris *et al.*, 1988).

HTA1–HTB1 synthetic dosage phenotypes

The pattern of viability of the single and double glycine substitution mutants was consistent with the disruption of interactions between histone H4 and the [H2A–H2B] dimers. We reasoned that if point mutations in the H4 tyrosines perturb these interactions, then altered dosage of the H2A and H2B genes might significantly affect the growth phenotype of the mutants. To test the effect of reduced H2A and H2B gene dosage, we deleted the *HTA1–HTB1* gene set encoding these proteins (Hereford *et al.*, 1979) by one-step gene disruption (see Materials and methods). Decreased dosage of *HTA1–HTB1* did not alter the temperature-dependent growth characteristics of either the wild-type or mutant H4 strains (data not shown). To test the effect of overexpression of histones H2A and H2B, strains expressing *hhf1-36* (Y72G), *hhf1-37* (Y88G) or *hhf1-39* (Y98H) were transformed with a high copy YEp24-derived plasmid expressing the *HTA1–HTB1* gene set and examined for their growth at restrictive and semi-permissive temperatures. Overexpression of *HTA1–HTB1* had no detectable effect on *hhf1-37* (Y88G) at either 34 or 37°C (data not shown). However, as can be seen in Figure 4, at a semi-permissive temperature of 34°C,

increased *HTA1–HTB1* gene dosage strongly inhibited the growth of *hhf1-36* (Y72G) cells, compared with expression of YEp24 alone. A slight inhibition was also detected with *hhf1-39* (Y98H) cells (Figure 4). These synthetic dosage phenotypes of high-copy *HTA1–HTB1* suggest a functional genetic interaction between [H2A–H2B] dimers and the Y72G and Y98H mutant histone H4 proteins (Kroll *et al*., 1996).

H4 tyrosine mutants are Spt⁻

Alterations in the relative ratio of the H3–H4 and H2A–H2B histone gene pairs can have strong effects on a variety of cell functions, including mitotic chromosome transmission (Meeks-Wagner and Hartwell, 1986; Smith and Stirling, 1988) and mRNA transcription (Clark-Adams *et al.*, 1988; Hirschhorn *et al*., 1992). These effects of histone gene stoichiometry are presumably mediated by changes in the composition of the chromatin through alterations in dimer–tetramer interactions. If the molecular defect in the H4 tyrosine mutants is in dimer–tetramer interactions, then these mutants should exhibit the same phenotypes as strains with altered gene ratios. To test this prediction, we examined the ability of the mutations to suppress Ty1 solo δ insertions. Insertions of Ty1 solo δ elements in the 5′ regions of the *HIS4* (*his4-912*δ) or *LYS2* (*lys2-128*δ) genes cause alterations in their transcription initiation start sites leading to non-functional transcripts. Mutations in *SPT* genes suppress these defects by restoring transcription of the affected genes (Simchen *et al*., 1984; Winston *et al.*, 1984; Fassler and Winston, 1988). Either overproduction or underproduction of histone dimer gene sets produces an Spt⁻ phenotype and restores gene expression (Clark-Adams *et al*., 1988).

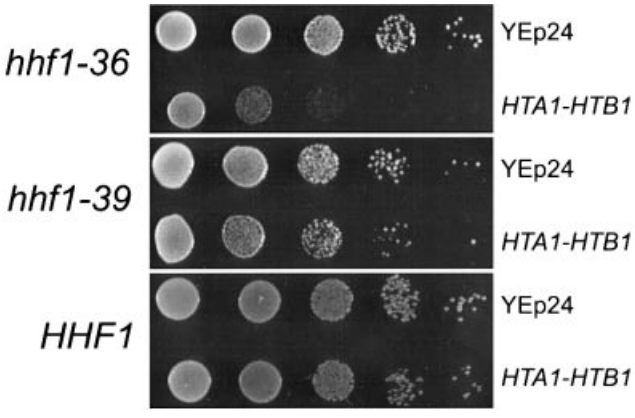

Fig. 4. Overexpression of H2A–H2B decreases the growth rate of *hhf1-36* (Y72G) and *hhf1-39* (Y98H) strains. Strain Y72G (*hhf1-36*) was transformed with either YEp24 (line 1) or *HTA1–HTB1* in YEp24 (line 2). Transformants were grown in SDC-URA liquid medium until log phase. Serial dilutions of cell suspensions, ranging from 1×10^5 down to 10 cells, were spotted onto SDC-ura plates and incubated at 34°C for 3 days. Lines 3 and 4 show the growth of Y98H (*hhf1-39*) cells transformed with either YEp24 or *HTA1–HTB1* in YEp24. Lines 5 and 6 show the growth of the wild-type *HHF1* cells transformed with either YEp24 or *HTA1–HTB1* on YEp24.

As shown in Figure 5, *hhf1-36* (Y72G), *hhf1-37* (Y88G) and *hhf1-39* (Y98H), but not *hhf1-40* (Y98W) or wild-type *HHF1*, were able to suppress *his4-912*δ and *lys2-128*δ mutations and support colony formation on SDC-HIS and SDC-LYS plates. All three alleles were strong suppressors of *his4-912*δ and weaker suppressors of *lys2-128*δ. The *hhf1-39* (Y98H) allele was the weakest suppressor of the three, and growth in medium lacking lysine was not observed until at least 4 days of incubation. Thus, substitution mutations in these H4 tyrosines each result in cells that display Spt⁻ phenotypes.

Histone H4 mutants are Sin⁻

A number of histone mutations, including altered stoichiometry of the dimer–tetramer gene sets, suppress the loss of transcriptional activation caused by mutations in genes encoding the SWI–SNF complex proteins, rendering regulated target genes SWI–SNF independent (Sin⁻) (Happel *et al*., 1991; Malone *et al.*, 1991; Hirschhorn *et al*., 1992; Kruger *et al.*, 1995). Since the H4 tyrosine mutations targeted the dimer–tetramer interface, we anticipated that they might have Sin⁻ phenotypes.

The *SUC2* gene encodes the enzyme invertase necessary for utilization of sucrose and raffinose as carbon sources. The transcriptional activation of *SUC2* depends on the function of the SWI–SNF complex to remodel the repressive chromatin structure at the *SUC2* promoter (Hirschhorn *et al*., 1992). Mutants in SWI–SNF complex genes, such as *snf2* or *snf5*, fail to remodel promoter chromatin structure and do not activate *SUC2* transcription. Deletion of the histone *HTA1–HTB1* locus generates an active chromatin structure over the *SUC2* promoter, thus bypassing the requirement for SWI–SNF complex function and activating transcription in *swi* and *snf* mutants (Hirschhorn *et al.*, 1992). We tested the tyrosine histone H4 mutants for Sin⁻ phenotypes by knocking out *SNF2* in the mutants using a *snf2::URA3* disruption allele. As shown in Figure 6A, none of the H4 alleles suppressed the growth defect of the *snf2* disruption on raffinose plates. Consistent with these results, there was also no increase in *SUC2* mRNA levels in the double mutants (Figure 6B).

We next examined the effect of the histone mutations

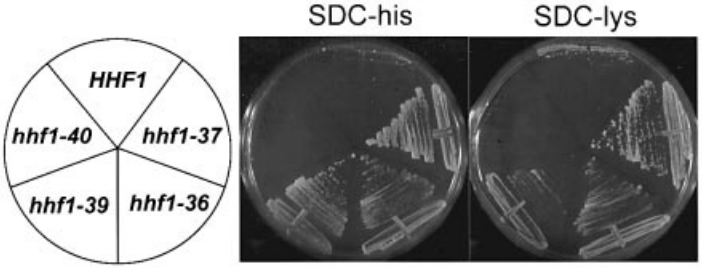

Fig. 5. Suppression of *his4-912*δ and *lys2-128*δ by histone H4 mutations. The wild-type and histone H4 mutant alleles were introduced by ectopic integration into a *his4-912*δ *lys2-128*δ strain and the growth was assayed on synthetic media lacking histidine and lacking lysine. After 5 days of incubation at 28°C, only the strains expressing *hhf1-36* (Y72G), *hhf1-37* (Y88G) and *hhf1-39* (Y98H) showed significant growth.

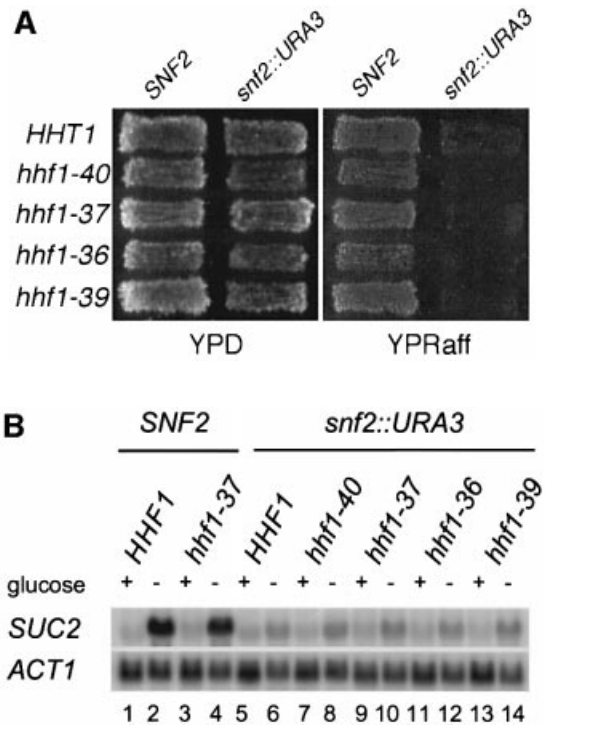

Fig. 6. Histone H4 mutations do not suppress the defect in *SUC2* transcription due to a *snf2::URA3* disruption. (**A**) Wild-type and histone H4 Tyr mutant strains, in *SNF2* and *snf2* backgrounds, were grown on complete media and then replica-plated onto media containing glucose or raffinose as carbon sources. Although all the strains were able to grow in the medium supplemented with glucose, only the *SNF2* strains grew in the raffinose medium. (**B**) mRNA levels of *SUC2* in the wild-type and histone H4 Tyr mutant cells grown under repressive (2% glucose) or inducing (0.02% glucose) conditions analyzed by Northern blot. Northern blots were probed with *SUC2* and *ACT1* probes.

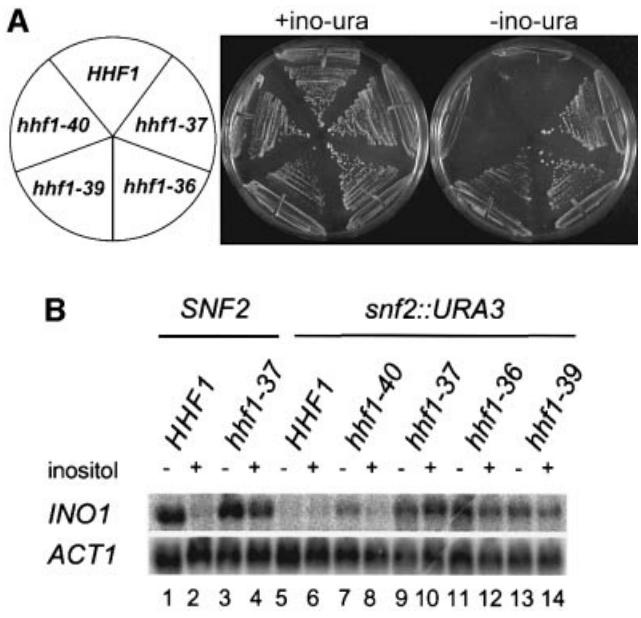

Fig. 7. Histone H4 mutations suppress the inositol auxotrophy due to a *snf2::URA3* disruption. (**A**) Growth of the wild-type H4 and mutant strains is shown for media lacking inositol or supplemented with 100 μM of myo-inositol. All the strains carried the *snf2::URA3* disruption. Wild-type *HHT1* and *hhf1-40* (Y98W) cells required inositol to grow, whereas *hhf1-36* (Y72G), *hhf1-37* (Y88G) and *hhf1-39* (Y98H) cells could grow without inositol in the medium. (**B**) Northern analysis of the *INO1* for the wild-type and isogenic H4 mutant strains in the *snf2* and *SNF2* backgrounds. mRNA levels are shown for cells grown under either repressive (100 μM myo-inositol) or inducing conditions (10 μM myo-inositol).

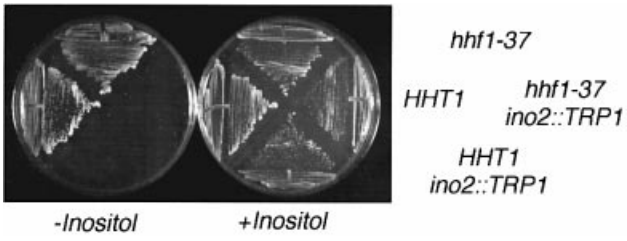

Fig. 8. Histone H4 mutants do not relieve the requirement for *INO2*. Growth of the wild-type *HHT1* and *hhf1-37* (Y88G) strains with either the wild-type *INO2* or the disrupted *ino2::TRP1* gene is shown after 6 days of incubation in synthetic media lacking inositol or supplemented with 100 μM of myo-inositol.

on *INO1* gene expression since it also requires the function of the SWI–SNF complex for activation (Peterson *et al.*, 1991). In contrast to the results at *SUC2*, *hhf1-36* (Y72G) and *hhf1-37* (Y88G) relieve the growth defect of *snf2* mutants on Ino$^-$ plates (Figure 7A). The *hhf1-39* (Y98H) allele also relieves repression, but more weakly (Figure 7A). Consistent with its Spt$^+$ phenotype, no suppression was observed for *hhf1-40* (Y98W). These results were confirmed by Northern blot analysis of *INO1* mRNA levels (Figure 7B). In the *SNF2* wild-type strain, the induction of the *INO1* mRNA by low inositol was ~14-fold (lanes 1 and 2). The isogenic *snf2* mutant shows about a 35-fold reduction in *INO1* transcription under derepressing conditions (lane 6). Under the same conditions, the *snf2* double mutants with either *hhf1-36* or *hhf1-37* increased *INO1* mRNA levels ~26-fold over the *snf2* single mutant (lanes 9 and 11). A more modest increase of 16-fold was observed for the *hhf1-39* mutant (lane 13). Increased *INO1* transcription was also observed under repressing conditions in the three histone mutant strains, resulting in only about a 1.5-fold difference between repressed and induced mRNA levels. Therefore, the histone H4 tyrosine mutations not only suppress mutations in *snf2*, but also relieve the repression caused by high levels of inositol in the medium (Hirsch and Henry, 1986).

We then examined the effect of the histone mutations on the positive regulators of *INO1*. The products of the *INO2* and *INO4* genes form a transcription factor complex that binds to the *INO1* promoter (Ambroziak and Henry, 1994; Ashburner and Lopes, 1995). As shown in Figure 8, the *hhf1-37* allele did not suppress an *ino2::TRP1* disruption for growth on media lacking inositol. Identical results were obtained with the other mutant alleles of H4 (data not shown). Consistent with this growth pattern, the levels of *INO1* mRNA in *ino2::TRP1* mutants were low both in wild-type and in *hhf1-37* cells (data not shown).

Histone H4 mutants alter chromatin structure at the INO1 locus

We next examined the chromatin structure of the *INO1* locus in wild-type histone and H4 mutant strains, in both wild-type *SNF2* and *snf2* mutant backgrounds. An autoradiograph of the results of a micrococcal nuclease footprint of the locus is shown in Figure 9A. In wild-type cells, the most significant difference between repressing

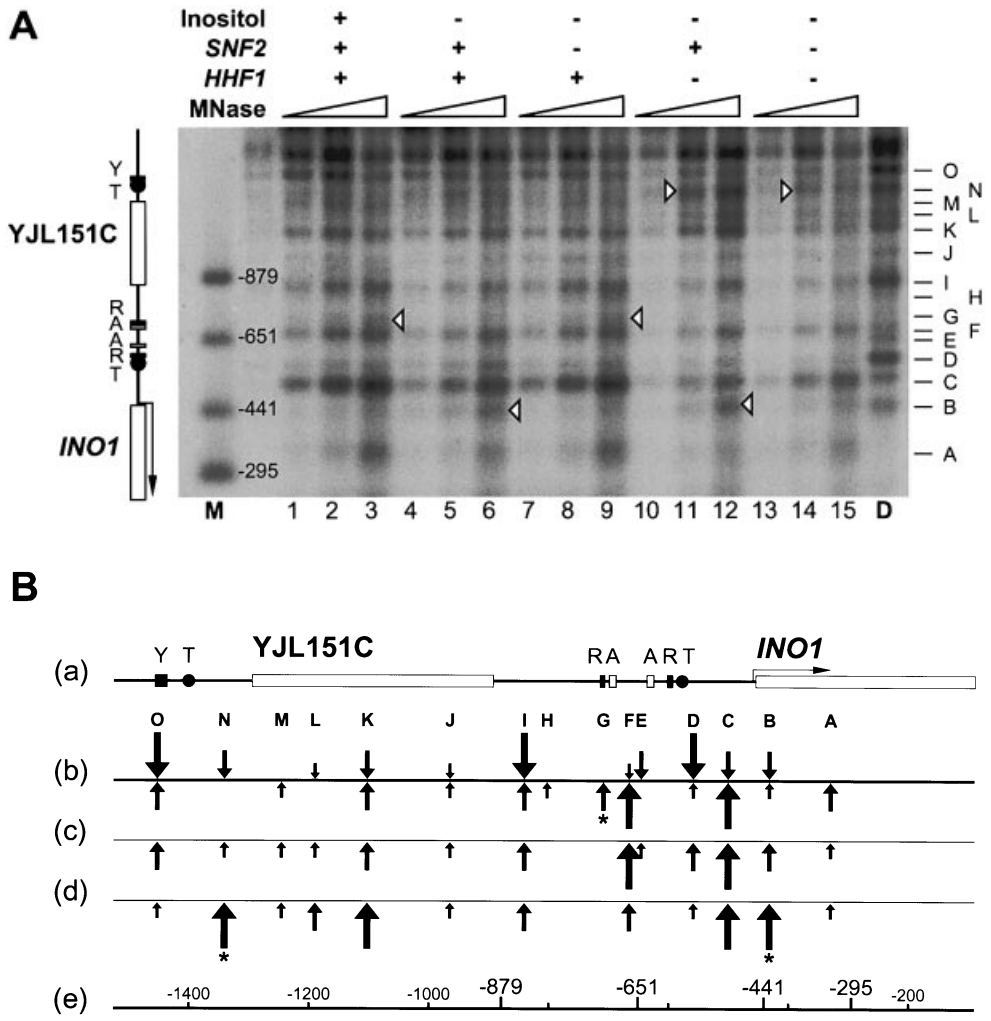

Fig. 9. Histone H4 mutations alter the chromatin structure at the *INO1* locus. (**A**) Autoradiograph of an indirect end-labeled blot of chromatin digests. Nuclei were partially digested with micrococcal nuclease and then purified DNA was digested to completion with *Bgl*II. The blot was probed with a radiolabeled *Afl*III–*Bgl*II fragment of 295 bp. The nuclease digestion patterns of chromatin are presented in lanes 1–15 as sets of three digests for each strain and growth condition. These are keyed at the top of the figure: inositol '+' indicates medium with 10 mM inositol and '–' indicates medium lacking inositol; *SNF2* '+' indicates wild-type *SNF2* and '–' indicates the *snf2::URA3* knockout allele; *HHF1* '+' indicates wild-type *HHF1* and '–' indicates the *hhf1-37* allele. The MNase ramps indicate increasing concentrations of enzyme in the digests. Lane M shows the position of restriction fragments that serve as internal molecular weight markers; the coordinates of the marker-cut sites are labeled relative to the *Bgl*II site located within the *INO1* coding sequence. Lane D shows the micrococcal nuclease digestion pattern of purified DNA. A diagram of the locus is shown at the left of the panel scaled to the coordinates of the autoradiograph image. The locations of the *INO1* gene and the YJL151C open reading frame are shown by the open boxes. The sequence features are labeled as follows: 'Y' for a 30 bp oligopyrimidine tract; 'T' for putative TATA box elements; 'R' for URS1 negative regulatory sites; and 'A' for *INO1* UAS promoter elements. The micrococcal nuclease-cut sites are labeled A–O along the right side of the panel. (**B**) Summary of changes in the chromatin structure at the *INO1* locus. Micrococcal nuclease digestion sites labeled A–O above the lines correspond to the bands labeled in (A). The relative intensity of the sites is reflected in the size of the arrows, with the larger arrows representing greater sensitivity to the nuclease. Line (a): a diagram of the locus representing the linear DNA sequence. Features are keyed as in (A). Line (b): downward arrows represent the cut sites in naked DNA, while upward arrows represent sites in the chromatin of either *HHF1 SNF2* cells under high inositol repressing conditions or *HHF1 snf2::URA3* cells. Line (c): the upward arrows represent sites in the chromatin of *HHF1 SNF2* cells induced by the absence of inositol. Line (d): the upward arrows represent sites in the chromatin for *hhf1-36* and *hhf1-37* histone H4 mutants, either *hhf1 SNF2* or *hhf1 snf2::URA3* both for repressing and inducing medium. Lane (e): the DNA coordinates relative to the *Bgl*II site within the *INO1* coding region. The positions of the four internal marker fragments are shown in larger type face.

(lanes 1–3) and inducing conditions (lanes 4–6) occurs at nuclease site G. Site G is one of the few digestion sites within the locus that is specific to chromatin templates, and it becomes accessible to nuclease only under repressing conditions (arrow, lane 3). In addition to this change, there is also a quantitative increase in the sensitivity of nuclease site B under inducing conditions (arrow, lane 6). Both these sites are functionally significant. Site G encompasses an upstream URS1 and a UAS_{INO} site known to be required for gene regulation both *in vivo* and *in vitro* (Lopes *et al.*, 1991; Ambroziak and Henry, 1994; Swift and McGraw, 1995). Site B covers the start site for *INO1* mRNA initiation, and a change in the chromatin structure of this region is consistent with a proposed positive downstream element suggested by genetic analysis (Swift and McGraw, 1995).

The *snf2::URA3* gene disruption blocks the formation of the active chromatin configuration at *INO1*. In the absence of Snf2p, the chromatin structure of the locus maintains the repressed state even under inducing conditions (lanes 7–9); site G remains accessible to nuclease (arrow, lane 9) and site B becomes relatively insensitive.

The effect of the *hhf1-37* allele on this structure is shown in lanes 13–15. Consistent with its Sin⁻ phenotype, the *hhf1-37* mutant establishes the active chromatin state at *INO1* even in the *snf2::URA3* disruption background. In particular, in the *hhf1-37 snf2::URA3* double mutant, site G now becomes resistant to micrococcal nuclease digestion even though it is sensitive in the *snf2::URA3* single mutant. Although only weakly apparent in Figure 9A, we conclude that site B also becomes more sensitive to digestion in the *hhf1 snf2* double mutant on the basis of additional experiments (data not shown). The results of micrococcal nuclease footprinting of *hhf1-36* chromatin were identical to those obtained for the *hhf1-37* mutants (data not shown).

In addition to these alterations that correlate with *SNF2* function, we also detected histone-dependent changes that may be unrelated to normal mechanisms of gene activation. In both *hhf1-37 SNF2* (lanes 10–12) and *hhf1-37 snf2::URA3* (lanes 13–15) strains, site N becomes strongly hypersensitive (arrows, lanes 11 and 14). This site is also hypersensitive in *hhf1-37* strains under repressing conditions (data not shown). Site N lies in the upstream promoter region of YJL151C, an open reading frame of unknown function. YJL151C encodes a 0.6 kb mRNA and its transcription is regulated coordinately with *INO1* (Hirsch and Henry, 1986; Dean-Johnson and Henry, 1989). However, the prominent digestion of site N appears to be specific for the histone mutants and does not correlate with inducing or repressing growth conditions. Thus, although the H4 tyrosine mutants do not have a global disruption of micrococcal nuclease ladders (Figure 3), the results presented here show that they do have at least two classes of chromatin defects: (i) defective interactions with SWI–SNF function and probably other chromatin regulatory proteins, and (ii) localized mutant-specific structural changes.

CDC phenotype of the mutants

The lethality of *hhf1-38* and *hhf1-41* plus the Ts⁻ phenotypes of the other H4 tyrosine mutants show that the histone dimer–tetramer interactions play essential roles in the cell. To begin to understand these essential pathways, we examined the Ts⁻ phenotype of the conditional mutants in greater detail. In principal, perturbing dimer–tetramer interactions might be expected to cause defects in at least two different major pathways: RNA transcription and DNA replication. Therefore, we asked whether the normal kinetics of cell division cycle (CDC) progression were affected in the tyrosine mutants at the restrictive temperature. Defects in DNA replication might be expected to cause a cell division cycle arrest at the G_2–M boundary by activating the DNA damage checkpoint regulatory system (Hartwell and Weinert, 1989; Weinert *et al.*, 1994). Alternatively, defects in transcription might lead to either a general growth arrest, or blocks at specific points in the division cycle that might depend on the proper expression of particular genes.

To assess the cell cycle pattern of the mutants, liquid cultures were grown at the permissive temperature until early log phase and then shifted to 37°C. Periodically after the temperature shift, cells were fixed and their cell cycle distribution assayed by flow cytometry. The DNA histograms for these measurements are shown in Figure 10.

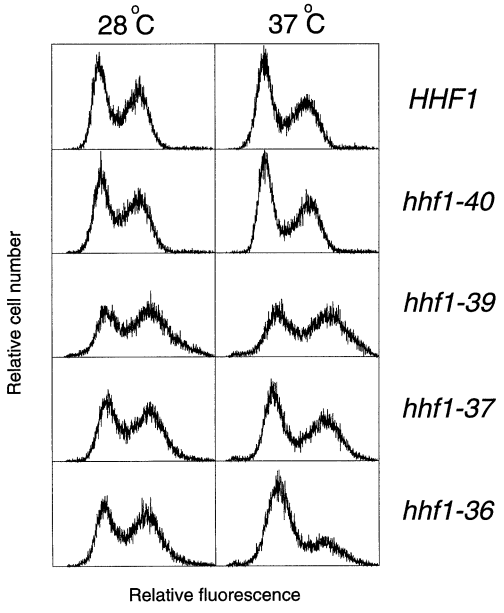

Fig. 10. DNA histograms of wild-type and H4 mutant cells at 28 and 37°C. Exponentially growing cultures of the wild-type and mutant cells were fixed and stained with propidium iodide. DNA content was measured by FACS analysis. The histograms of DNA contents are shown for wild-type and mutant cell populations growing exponentially at 28°C, or shifted to 37°C for 5 h.

As expected, the growth rate of the *hhf1-40* (Y98W) mutant was wild-type and the cell cycle distribution of the population was identical at the permissive and restrictive temperatures. On the other hand, cells expressing *hhf1-37* (Y88G) or *hhf1-39* (Y98H) grew very slowly at the restrictive temperature. However, the DNA histograms did not show any accumulation of cells in any specific stage of the cell cycle. In contrast, *hhf1-36* (Y72G) cells rapidly arrested cell division at 37°C with a characteristic terminal morphology consisting of unbudded cells with a single nucleus and 1C DNA content.

The G_1 arrest of *hhf1-36* (Y72G) was confirmed using synchronous cultures. Early G_1 cells were isolated by centrifugal elutriation and split into two cultures, one grown at 28°C and the other at 37°C. As can be seen in Figure 11A, at the restrictive temperature *hhf1-36* cells arrested in the first division cycle with unreplicated DNA. Cells remained tightly arrested even after 5 h at 37°C, at which time the cells maintained at 28°C were approximately at the end of the second division cycle. An isogenic control strain expressing the wild-type *HHF1* gene divided synchronously at both the permissive and restrictive temperature (Figure 11B). These results indicate that the rate-limiting growth step in the H4 tyrosine replacement mutants is not likely to be in DNA replication. Rather, the division cycle phenotypes suggest a more global defect in gene expression for *hhf1-37* and *hhf1-39* mutants, and a specific G_1 arrest in the case of *hhf1-36*.

The H4-dependent step in *hhf1-36* cells was mapped relative to 'Start,' the G_1–S phase transition, through reciprocal shift experiments using α-factor and the restrictive temperature. First, early G_1 cells were selected by centrifugal elutriation, arrested at 37°C for 2.5 h, and then returned to 28°C. As shown in Figure 12, cells shifted into medium containing α-factor remained arrested in G_1,

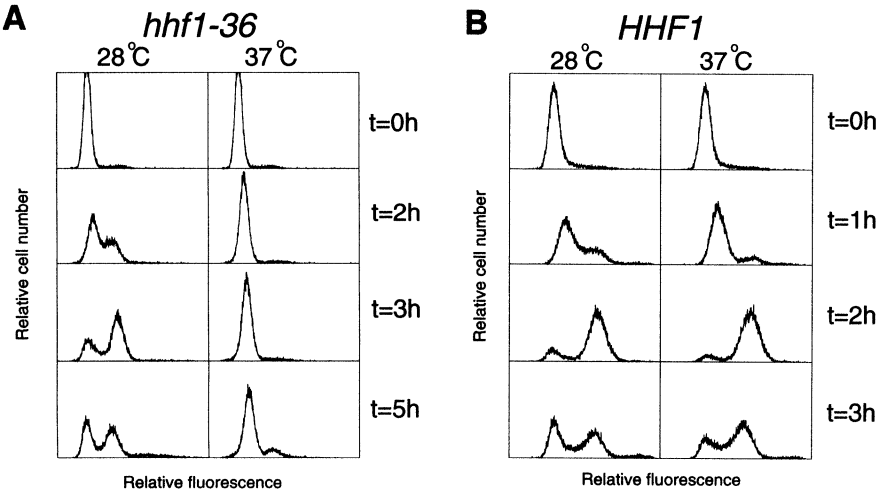

Fig. 11. Mutant *hhf1-36* (Y72G) cells arrest in G_1. DNA histograms are shown for *hhf1-36* (Y72G) cells (**A**) and wild-type cells (**B**) synchronized by centrifugal elutriation and grown at either 28 or 37°C.

while those shifted into medium without α-factor resumed progression through the division cycle. In the complementary experiment, early G_1 cells were first arrested with α-factor at 28°C for 2.5 h. They were then either shifted to 37°C or kept at 28°C, and washed free of α-factor. Cells at 28°C resumed normal cell cycle progression when the α-factor was removed, while cells shifted to 37°C remained arrested in G_1 (Figure 12). These results show that the G_1 histone H4-dependent step defined by *hhf1-36* and the α-factor-dependent step at Start are interdependent.

G_1 cyclin gene expression in hhf1-36

This interdependence of histone H4 function and Start suggested that the expression of one or more regulatory components of the G_1–S phase transition might be blocked in *hhf1-36* cells. We first examined the expression of the G_1 cyclin genes *CLN1*, *CLN2* and *CLN3*, because the proteins produced are functionally unstable and hence a failure in their transcription would result in a rapid first cycle cell division arrest (Richardson *et al.*, 1989; Cross, 1990; Wittenberg *et al.*, 1990). Northern analysis was used to quantify mRNA in cells synchronized by centrifugal elutriation and grown at either 28 or 37°C for 3 h (Figure 13). While the mRNA levels of *CLN1* and *CLN2* peaked at ~2 h for cells grown at 28°C, they were virtually absent in cells grown at 37°C. The levels of *CLN3* mRNA were also lower in the cells at 37°C than those at 28°C. These results suggested that the G_1 arrest of *hhf1-36* cells was due to the reduced expression of the G_1 cyclin genes. We confirmed this hypothesis by transforming these cells with a plasmid expressing a dominant mutant allele of the *CLN2* gene (*CLN2-4*) that encodes a hyperstable protein. The *CLN2-4* allele (generously provided by Drs Lanker and Wittenberg) encodes a carboxy-terminal truncation of Cln2p that is missing sequences that target rapid degradation (Rogers *et al.*, 1986). Expression of *CLN2-4* suppresses the G_1 arrest phenotype of *hhf1-36*, and synchronized *hhf1-36 CLN2-4* cells are able to complete the G_1–S phase transition at the restrictive temperature (Figure 14). Similar results were obtained with *CLN2* under the control of the *GAL1* promoter; *hhf1-36* p*GAL-CLN2* cells grown at 37°C in the presence of galactose failed to arrest in G_1, while those grown in raffinose

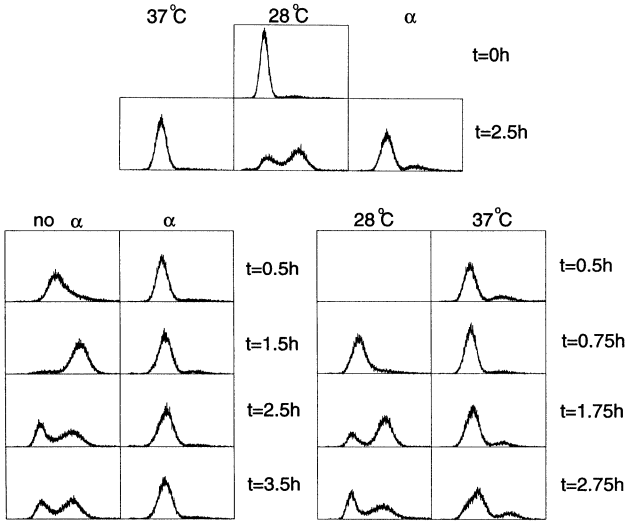

Fig. 12. The Ts^- step for *hhf1-36* cells is interdependent with α-factor arrest. (**A**) DNA histograms are shown for *hhf1-36* (Y72G) cells synchronized by centrifugal elutriation ($t = 0$) and then incubated at 28 or 37°C, with or without α-factor for 2.5 h (upper panel). Cells from the 37°C arrested culture were then shifted to medium at 28°C containing either α-factor or no pheromone and grown for a further 5 h (left lower panel). Cells arrested by α-factor for 2.5 h were then shifted to 37°C for 30 min (lower right panel, $t = 0.5$). The α-factor was then washed off and cells were allowed to progress at either 28°C (right lower panel, left plots) or 37°C (right plots).

arrested as expected (data not shown). However, *CLN2-4* is not sufficient to suppress *hhf1-36* for viability at 37°C. At the restrictive temperature they progress slowly through the cell division cycle and stop dividing after a few cycles without a unique terminal morphology. Thus, it is likely that *hhf1-36* cells have additional defects in essential functions besides their failure to activate transcription of the G_1 cyclin genes.

Since the transcriptional activation of the *CLN1* and *CLN2* genes as well as the post-translational activity of *CLN3* depend on activation of the *SWI4* and *SWI6* genes (Nasmyth and Dirick, 1991; Ogas *et al.*, 1991), we measured *SWI4* and *SWI6* mRNA levels in *hhf1-36* cells. As shown in Figure 15, both *SWI4* and *SWI6* mRNA levels were greatly reduced in exponentially growing

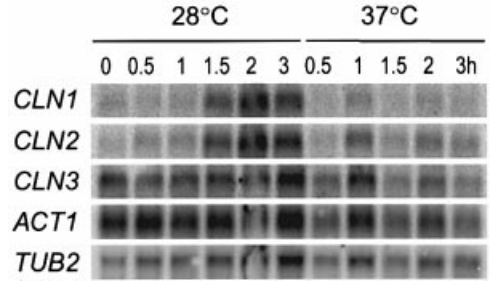

Fig. 13. Northern analysis of *hhf1-36* (Y72G) cells. The mRNA levels of the *CLN1*, *CLN2*, *CLN3*, *ACT1* and *TUB2* are shown for cells synchronized by centrifugal elutriation and grown at 28 or 37°C for the indicated periods of time.

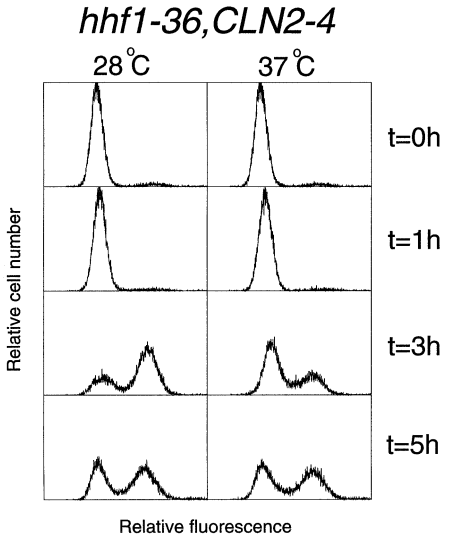

Fig. 14. The hyperstable *CLN2-4* allele suppresses the G_1 arrest of *hhf1-36* (Y72G) cells. DNA content assessed by flow cytometry is shown for *hhf1-36 CLN2-4* cells synchronized by centrifugal elutriation ($t = 0$) after various times at 28 or 37°C.

cultures shifted to 37°C, suggesting that the reduction in cyclin expression might be an indirect effect of the inhibition of *SWI4* and *SWI6* transcription. Together, these results show that dimer–tetramer interactions in the histone core octamer play essential roles in gene expression, and that the contacts mediated by H4 Tyr72 have a unique role in transcriptional activation of the *CLN1*, *2* and *3* and the *SWI4* and *6* division cycle regulatory pathway.

Discussion

The site-directed mutational analysis reported here shows that the three tyrosine residues at positions 72, 88 and 98 in the H4 histone fold are essential for function. The single substitution allele *hhf1-38* (Y98G) and the double substitution allele *hhf1-41* (Y72G+Y88G), are both lethal. Single substitution mutants with either *hhf1-36* (Y72G), *hhf1-37* (Y88G) or *hhf1-39* (Y98H) are temperature sensitive, showing defects in transcription and cell proliferation. These tyrosines were selected for mutation because of their predicted roles in mediating interactions between histone H4 and the [H2A–H2B] dimer subunits. Several lines of genetic evidence are consistent with this prediction. First, the pattern of lethal tyrosine substitutions is consistent with the physical structure of the octamer and the

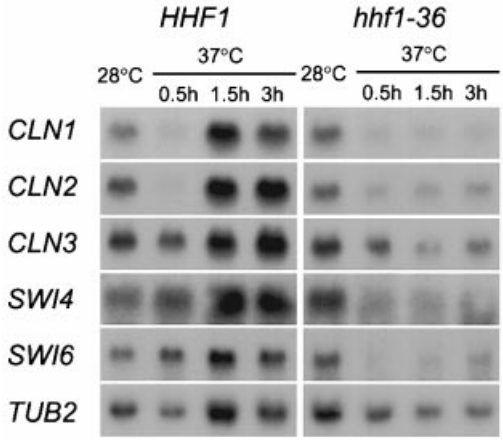

Fig. 15. *SWI4* and *SWI6* transcription is down-regulated in the *hhf1-36* (Y72G) cells grown at 37°C. Total RNA was prepared from exponentially dividing cultures grown at 28 or 37°C.

interactions of each H4 with each dimer. Second, the mutants have the Spt$^-$ and Sin$^-$ phenotypes expected for altered dimer–tetramer interactions (Clark-Adams *et al.*, 1988; Hirschhorn *et al.*, 1992; Kruger *et al.*, 1995). Third, overexpression of histones H2A and H2B causes a synthetic dosage lethality in the case of *hhf1-36* (Y72G) and growth inhibition in the case of *hhf1-39* (Y98H), suggesting a genetic interaction between [H2A–H2B] dimer subunits and the mutant H4 proteins. One interpretation of this dosage lethality is that histone $[H3–H4]_2$ tetramers might interact with [H2A–H2B] dimers to form a proportion of aberrant nucleosomes when the H4 tyrosines in the dimer–tetramer interface are mutated. An increased dosage of [H2A–H2B] dimers then might drive an increased proportion of complexes into functionally defective nucleosomes.

The phenotypes of the H4 tyrosine substitution mutants reveal striking consequences for gene transcription, both positive and negative. Previous studies have shown that the N-terminal domains of histones H3 and H4 may have both positive and negative roles in gene regulation (Durrin *et al.*, 1991; Mann and Grunstein, 1992; Hecht *et al.*, 1995). However, mutations in the histone fold domains have only derepressed gene expression, presumably by disrupting a repressive chromatin structure (Hirschhorn *et al.*, 1995; Kruger *et al.*, 1995). The positive transcription phenotypes seen with the mutants reported here are in agreement with these previous studies and are consistent with the model of *SWI*, *SNF* and *SIN* gene function (Winston and Carlson, 1992; Peterson and Tamkun, 1995). For example, at *INO1* the tyrosine substitution mutants bypass the normal requirement for the SWI–SNF complex in remodeling chromatin structure, but do not relieve the requirement for the gene-specific transcriptional activators *INO2* and *INO4*.

The negative transcriptional effects of *hhf1-36* are unusual and important in that they repress the expression of genes critical for cell division cycle control during G_1. The phenotypes of *hhf1-36* cells are similar to those of mutants in the *CDC68* (*SPT16*) gene (Rowley *et al.*, 1991; Lycan *et al.*, 1994). Like *hhf1-36*, *cdc68* mutations suppress the transcription defects of Ty1 δ-insertions at *his4-912*δ and *lys2-128*δ (Malone *et al.*, 1991). This Spt$^-$ phenotype is likely to be the result of altered histone

dimer–tetramer stoichiometry because of the reduced transcription of *HTA1* and *HTB1* in *cdc68* cells (Xu *et al.*, 1993). At the restrictive temperature, *cdc68* mutants also arrest in late G_1 as a consequence of low levels of *CLN1*, *CLN2*, *CLN3*, *SWI4* and *SWI6* mRNA (Rowley *et al.*, 1991; Lycan *et al.*, 1994). For both *cdc68* and *hhf1-36* mutants, expression of dominant *CLN2* alleles suppresses the G_1 arrest but not the Ts^- phenotype, suggesting that the transcription of other essential genes is also defective. It is unlikely that *hhf1-36* acts indirectly through *CDC68* expression since *cdc68* mutants show a marked decrease in *ACT1* mRNA at the restrictive temperature (Rowley *et al.*, 1991) while *hhf1-36* mutants do not (Figure 13). However, given the strong genetic links between *CDC68* function and chromatin structure (Xu *et al.*, 1993; Lycan *et al.*, 1994), one target of Cdc68p might be the regulation of histone dimer–tetramer interactions. In such a case, the effect of *cdc68* mutations and *hhf1-36* could have similar consequences for chromatin structure, producing similar phenotypes in the mutants.

The transcriptional activation of *CLN1* and *CLN2* is thought to be the rate-limiting step in the entry of cells into the division cycle (Tyers *et al.*, 1993; Dirick *et al.*, 1995). The activation of *CLN2* is complex and is mediated through two *cis*-acting upstream activation sites (UAS1 and UAS2) in the promoter of the gene (Cross *et al.*, 1994; Stuart and Wittenberg, 1994). Transcriptional activation through these UAS elements depends directly on *SWI4* in at least two ways: (i) as a complex with Swi4p and Swi6p to form the transcription activation complex SBF which binds to multiple Swi4–Swi6 cell cycle box (SCB) DNA elements located within UAS1 (Nasmyth and Dirick, 1991; Ogas *et al.*, 1991); and (ii) in a less well understood mechanism involving UAS2 that is independent of SCB sites (Cross *et al.*, 1994; Stuart and Wittenberg, 1994). Expression of *SWI4* and *SWI6*, in turn, can be stimulated by the activity of the G_1 Cln/Cdc28p kinase (Taba *et al.*, 1991; Dirick *et al.*, 1992). Cellular regulation of *CLN2* transcription is controlled by parallel *trans*-acting pathways. One pathway involves *CLN3* (Stuart and Wittenberg, 1995), apparently through the activation of SBF bound at the *CLN2* promoter by the Cln3p/Cdc28p kinase (Dirick *et al.*, 1995; Koch *et al.*, 1996). A less well understood parallel pathways involves *SIT4* and *BCK2* (Di Como *et al.*, 1995). Because of these interlocking regulatory links, we do not currently know the primary transcriptional defects in *hhf1-36* chromatin. In principle, the loss of *CLN1*, *2* and *3* and *SWI4* and *6* gene transcription in *hhf1-36* mutants could result from either a direct repression through the chromatin structure at the promoter of one or more of the genes involved, or an indirect effect through the derepression of an unknown transcriptional repressor. At present we cannot distinguish between these two models. Nevertheless, the important role of chromatin structure in the control of G_1 cyclin expression is clearly established by the *hhf1-36* mutant.

It is striking that the histones also participate in the regulation of the G_2–M cell cycle transition. Using a screen for synthetic lethal mutants, Ma *et al.* (1996) recently uncovered genetic interactions between the N-terminal domains of histones H3 and H4 and regulators of Swe1p, the kinase responsible for the phosphorylation of Cdc28p that controls a morphogenetic checkpoint at the G_2–M transition (Lew and Reed, 1995). Our finding that histone dimer–tetramer subunit interactions also affect the G_1–S transition, through expression of the G_1 cyclins, suggests that the regulatory components of the cell division cycle may have evolved to depend on multiple aspects of chromatin structure. The immediate challenge for future experiments will be to identify the primary targets of the *hhf1-36* chromatin defect from among the interlocking genes in the cyclin regulatory circuit, and to discriminate between direct and indirect mechanisms of repression.

Materials and methods

Strains and plasmids

Escherichia coli strains JM109 (*recA*1 *supE*44 *endA*1 *hsdR*17 *gyrA*96 *relA*1 *thi* Δ(*lac-proAB*) F′[*traD*36 *proAB*$^+$ *lacI*^{q} *lacZ*ΔM15]) and BMH 71-18 (*mutS thi supE* Δ(*lac-proAB*) *mutS::*Tn*10* F′[*proAB*$^+$ *lacI*^{q} *lacZ*ΔM15]) were used in the oligonucleotide-directed mutagenesis. Strain JA221 [*lacY leuB*6 Δ*trpE*5 *recA*1 *hsd*(r_k^- m_k^+)] was used for transformation of ligations requiring selection for the *LEU2* gene. Strain DH5α [*supE*44 Δ*lac*U169 (ϕ80 *lacZ*ΔM15) *hsdR*17 *recA*1 *endA*1 *gyrA*96 *thi-1 relA*1] was used for all other bacterial transformations.

The genotypes of the yeast strains used in this work are shown in Table I. Strain MX4-22A was used as parental strain to construct the histone H4 mutant alleles by ectopic integration at the *LEU2* locus. Strain MSY748 was used for testing Spt^- phenotypes and was obtained by crossing A970-3A with MSY423. S288C (*MAT*α *gal2 mal*) was used for α-factor production. Plasmid pMS329 is a *CEN4/ARS1/URA3/SUP11* vector containing the wild type *HHT1* and *HHF1* genes (Megee *et al.*, 1990). Plasmid pMS347 is a *LEU2/CEN4/ARS1* vector containing *HHT1* and a unique *Bam*HI site for the insertion of fragments carrying derivatives of *HHF1* (Megee *et al.*, 1990). Mutated histone H4 *Bam*HI fragments produced by oligonucleotide-directed mutagenesis were subcloned into pMS347 to create plasmids pMS337 (*HHF1*), pMS363 (*hhf1-36*), pMS364 (*hhf1-37*), pMS365 (*hhf1-38*), pMS366 (*hhf1-39*), pMS367 (*hhf1-40*) and pMS368 (*hhf1-41*). Plasmid TRT1 was kindly provided previously by L.Hereford (Hereford *et al.*, 1979).

Media

YPD, YNB, SC, inositol and 5-FOA media were made as described by Rose *et al.* (1990) and MV medium was prepared as described by Hereford *et al.* (1981). Plates for testing carbon source requirements included antimycin A (Sigma) at a final concentration of 1 μg/ml (Carlson *et al.*, 1981). For *INO1* expression in liquid culture, cells were grown in YNB medium (induced) or YNB plus 100 μM inositol (repressed).

Oligonucleotide-directed mutagenesis

The Altered Sites™ *in vitro* mutagenesis system (Promega) was used to produce the mutant alleles of histone H4. A 405 bp *Bam*HI fragment bearing wild-type copy I histone H4 was cloned into the phagemid vector pALTER-1. Mutant H4 sequences were confirmed by DNA sequencing.

Ectopic integrations

Histone H4 alleles. The 2.1 kb *Eco*RI–*Hin*dIII fragments containing wild-type *HHT1* and mutant alleles of *HHF1* were subcloned from pMS347-derived plasmids into the integrating vector pRS305 between the *Eco*RI and *Hin*dIII sites. The resulting plasmids were linearized with *Hpa*I to target the integration to the *LEU2* locus and used to transform yeast strains MX4-22A and MSY748. Integration was verified by Southern blot analysis.

CLN2 alleles. Plasmids pUC18-HIS2-CLN2-4 and YIpG2- GAL::CLN2 were a gift from S.Lanker and C.Wittenberg. A 3.7 kb *Sal*I–*Eco*RI fragment from pUC18-HIS2-CLN2-4 containing the *CLN2-4* allele was cloned between the *Sal*I and *Eco*RI sites of pRS306, and the resulting plasmid was transformed into yeast strain MSY781. For the *GAL::CLN2* integration, an *Eco*RI–*Bam*HI fragment from YIpG2-GAL::CLN2 was transferred to pRS306. Integration was targeted to the *URA3* locus by digestion of the plasmid DNA with *Cla*I and then used to transform MSY781. Integration was verified by Southern blot analysis.

Table I. Strain list

Strain	Genotype	H4 mutation
MX4-22A	*MAT***a** Δ(*HHT1 HHF1*) Δ(*HHT2 HHF2*) *leu2-3,112 lys2*Δ*201 ura3-52* pMS329[*URA3 HHT1 HHF1*]	WT
A970-3A	*MAT***a** *his4-912*δ *lys2-128*δ *ura3-52*	WT
MSY423	*MAT*α *leu2-3,112 ura3-52* Δ(*HHT1 HHF1*) Δ(*HHT2 HHF2*) pMS329[*URA3 HHT1 HHF1*]	WT
MSY623	*MAT***a** Δ(*HHT1 HHF1*) Δ(*HHT2 HHF2*) *LEU2*::(*HHT1 HHF1*) *lys2*Δ*201 ura3-52*	WT
MSY624	*MAT***a** Δ(*HHT1 HHF1*) Δ(*HHT2 HHF2*) *LEU2*::(*HHT1 hhf1-40*) *lys2*Δ*201 ura3-52*	Y98W
MSY625	*MAT***a** Δ(*HHT1 HHF1*) Δ(*HHT2 HHF2*) *LEU2*::(*HHT1 hhf1-39*) *lys2*Δ*201 ura3-52*	Y98H
MSY626	*MAT***a** Δ(*HHT1 HHF1*) Δ(*HHT2 HHF2*) *LEU2*::(*HHT1 hhf1-37*) *lys2*Δ*201 ura3-52*	Y88G
MSY781	*MAT***a** Δ(*HHT1 HHF1*) Δ(*HHT2 HHF2*) *LEU2*::(*HHT1 hhf1-36*) *lys2*Δ*201 ura3-52*	Y72G
MSY735	*MAT***a** Δ(*HHT1 HHF1*) Δ(*HHT2 HHF2*) *LEU2*::(*HHT1 hhf1-41*) *lys2*Δ*201 ura3-52* pMS329[*URA3 HHT1 HHF1*]	Y72G-Y88G/WT
MSY737	*MAT***a** Δ(*HHT1 HHF1*) Δ(*HHT2 HHF2*) *LEU2*::(*HHT1 hhf1-38*) *lys2*Δ*201 ura3-52* pMS329[*URA3 HHT1 HHF1*]	Y98G/WT
MSY743	*MAT***a** Δ(*HHT1 HHF1*) Δ(*HHT2 HHF2*) *LEU2*::(*HHT1 HHF1*) *lys2*Δ*201 ura3-52 snf2::URA3*	WT
MSY744	*MAT***a** Δ(*HHT1 HHF1*) Δ(*HHT2 HHF2*) *LEU2*::(*HHT1 hhf1-40*) *lys2*Δ*201 ura3-52 snf2::URA3*	Y98W
MSY749	*MAT***a** Δ(*HHT1 HHF1*) Δ(*HHT2 HHF2*) *LEU2*::(*HHT1 hhf1-37*) *lys2*Δ*201 ura3-52 snf2::URA3*	Y88G
MSY752	*MAT***a** Δ(*HHT1 HHF1*) Δ(*HHT2 HHF2*) *LEU2*::(*HHT1 hhf1-39*) *lys2*Δ*201 ura3-52 snf2::URA3*	Y98H
MSY807	*MAT***a** Δ(*HHT1 HHF1*) Δ(*HHT2 HHF2*) *LEU2*::(*HHT1 hhf1-36*) *lys2*Δ*201 ura3-52 snf2::URA3*	Y72G
MSY748	*MAT*α Δ(*HHT1 HHF1*) Δ(*HHT2 HHF2*) *his4-912*δ *lys2-128*δ *leu2-3,112 ura3-52* pMS329[*URA3 HHT1 HHF1*]	WT
MSY764	*MAT*α Δ(*HHT1 HHF1*) Δ(*HHT2 HHF2*) *LEU2*::(*HHT1 HHF1*) *his4-912*δ *lys2-128*δ *ura3-52*	WT
MSY765	*MAT*α Δ(*HHT1 HHF1*) Δ(*HHT2 HHF2*) *LEU2*::(*HHT1 hhf1-40*) *his4-912*δ *lys2-128*δ *ura3-52*	Y98W
MSY767	*MAT*α Δ(*HHT1 HHF1*) Δ(*HHT2 HHF2*) *LEU2*::(*HHT1 hhf1-37*) *his4-912*δ *lys2-128*δ *ura3-52*	Y88G
MSY769	*MAT*α Δ(*HHT1 HHF1*) Δ(*HHT2 HHF2*) *LEU2*::(*HHT1 hhf1-39*) *his4-912*δ *lys2-128*δ *ura3-52*	Y98H
MSY798	*MAT*α Δ(*HHT1 HHF1*) Δ(*HHT2 HHF2*) *LEU2*::(*HHT1 hhf1-36*) *his4-912*δ *lys2-128*δ *ura3-52*	Y72G
MSY828	*MAT***a** Δ(*HHT1 HHF1*) Δ(*HHT2 HHF2*) *LEU2*::(*HHT1 hhf1-36*) *lys2*Δ*201 URA3::pGAL-CLN2*	Y72G
MSY830	*MAT***a** Δ(*HHT1 HHF1*) Δ(*HHT2 HHF2*) *LEU2*::(*HHT1 hhf1-36*) *lys2*Δ*201 ura3-52 URA3*::CLN2-4	Y72G
MSY869	*MAT***a** Δ(*HHT1 HHF1*) Δ(*HHT2 HHF2*) *LEU2*::(*HHT1 HHF1*) *lys2*Δ*201 trp1-289 ura3-52*	WT
MSY870	*MAT***a** Δ(*HHT1 HHF1*) Δ(*HHT2 HHF2*) *LEU2*::(*HHT1 hhf1-37*) *lys2*Δ*201 trp1-289 ura3-52*	Y88G
MSY881	*MAT***a** Δ(*HHT1 HHF1*) Δ(*HHT2 HHF2*) *LEU2*::(*HHT1 HHF1*) *lys2*Δ*201* trp1-289 *ura3-52 ino2::TRP1*	WT
MSY880	*MAT***a** Δ(*HHT1 HHF1*) Δ(*HHT2 HHF2*) *LEU2*::(*HHT1-hhf1-37*) *lys2*Δ*201 trp1-289 ura3-52 ino2::TRP1*	Y88G

Gene disruptions

SNF2. A 1.1 kb fragment spanning bases 3054–4145 of the *SNF2* gene was amplified by PCR and cloned between the *Bam*HI and *Xba*I sites of the integrating plasmid pRS306. The plasmid was linearized by digestion with *Nru*I that cuts in the *SNF2* fragment to target the knockout to the *SNF2* gene. Integration was verified by Southern blot analysis.

INO2. A linear 1.9 kb *Sma*I–*Sal*I fragment from pMN118 (Nikoloff and Henry, 1994), provided by P.McGraw and S.Henry, containing *TRP1* as selectable marker was used to disrupt the *INO2* locus. Disruption was verified by Southern blot.

HTA1–HTB1. A 3.2 kb *Eco*RI–*Hpa*I linear fragment from pUC9-Δtrt1::URA3 (Norris and Osley, 1987), provided by M.A.Osley, was used to transform strains MSY623, MSY625, MSY626 and MSY781. Ura^+ transformants were subjected to Sourthern blot analysis to confirm deletion of the *HTA1–HTB1* locus.

Synchronized cultures

Cells in early G_1 were collected by elutriation (Gordon and Elliot, 1977) and split into two equal fractions. One was resuspended in fresh medium at 28°C and the other at 37°C. Samples of 5×10^6 cells were removed from both cultures at 30 min intervals and analyzed for DNA content and cell morphology to monitor the cell cycle progression. DNA content was measured by flow cytometry after propidium iodide staining, and morphology was assessed by microscopic examination of cells stained with 4′,6-diamidino-2- phenylindole (DAPI, Sigma) (Smith, 1991). For reciprocal-shift experiments, early G_1 cells were collected by elutriation and resuspended at 3×10^6 cells/ml in fresh MV medium containing α-factor and grown until cells in a control culture without α-factor reached the end of S phase. Cells were then collected by filtration, washed twice with MV medium, and resuspended in fresh MV medium pre-warmed at either 28 or 37°C. In the reciprocal experiment, cell cultures arrested at the restrictive temperature (37°C) were split into two parts, shifted to the permissive temperature (28°C), and α-factor was added to one of the cultures.

RNA analysis

Total RNA was extracted from cells grown to a density of 5×10^6–1×10^7 cells/ml. Ten μg of total RNA were electrophoresed in a formaldehyde–agarose gel (1% agarose) and then transferred to a nitrocellulose membrane. Nucleic acid probes for hybridization were: *SUC2*, a 772 bp fragment amplified by PCR; *INO1*, a 0.6 kb *Bgl*II–*Pvu*II fragment from plasmid pJH318 (Hirsch and Henry, 1986) provided by S.Henry; *CLN1*, a 1.2 kb *Eco*RI–*Pvu*II fragment from plasmid pGAL-CLN1 (a gift from F.Cross); *CLN2*, a 1.6 kb *Bam*HI–*Xho*I fragment from plasmid YIPG2 (a gift from C.Wittenberg); *CLN3*, a 1.8 kb *Bam*HI fragment from plasmid pW16 (a gift from F.Cross); *SWI4*, a 718 bp fragment amplified by PCR and cloned into pUC19 vector; *SWI6*, a 789 bp fragment PCR amplified and cloned into pUC19 vector; *ACT1*, a 1.1 kb *Xho*I–*Hin*dIII fragment from pRB147 plasmid (Shortle *et al*., 1984); and *TUB2*, a *Bst*EII fragment from plasmid pDB55 (provided by D.Burke). Hybridization was done at 42°C overnight in 50% formamide, 5× SSC, 0.1% SDS and 8% dextran sulfate.

Micrococcal nuclease digestion

Chromatin was prepared from wild-type and *hhf1-36* (Y72G) cells in early log-phase growth. Nuclei were isolated as described previously (Nelson and Fangman, 1979) using Zymolyase (ICN Biomedicals, Inc; 2 mg per 6×10^9 cells) for spheroplasting. Cells were lysed in 18% Ficoll, 0.02 M PIPES (pH 6.3), 0.5 mM $CaCl_2$, 1 mM phenylmethylsulfonyl fluoride (PMSF) with five strokes in a Dounce homogenizer. Nuclei were digested with micrococcal nuclease (Sigma) in 1.1 M sorbitol, 0.02 M PIPES (pH 6.3), 0.5 mM $CaCl_2$ (SPC) at 37°C for 5 min in four aliquots containing 1, 3, 10 and 30 U/ml of enzyme (Worthington units). Reactions were stopped by adding EDTA and SDS at final concentrations of 20 mM and 1% respectively. Digests were extracted four times with phenol:chloroform (1:1), and nucleic acids were precipitated for 30 min at –20°C with ethanol. The precipitate was redissolved in TE buffer (10 mM Tris, pH 7.5 and 1 mM EDTA, pH 8.0), adjusted to a final concentration of 0.3 M sodium acetate, treated with 200 μg/ml RNase I (Sigma) for 30 min at 37°C, and reprecipitated. For analysis of micrococcal nuclease ladders, samples of 10 μg of DNA were resolved by electrophoresis in each lane of a 1.2% agarose gel and stained with 50 μg/ml of ethidium bromide (Sigma).

The chromatin structure of the *INO1* locus was analyzed by indirect end labeling and mapped relative to the *Bgl*II site located within the *INO1* coding sequence. This *Bgl*II site is positioned 461 bp 3′ to the *INO1* mRNA start site at base pair 135 171 in the complete DNA sequence of chromosome X (Galibert *et al.*, 1996). The DNA sequence coordinates used in this work are based on the chromosome X sequence file ftp://genome-ftp.stanford.edu/yeast/genome_seq/chrx/chrx_745443.ascii deposited on 24 April 1996 in the *Saccharomyces* Genome Database, Department of Genetics, School of Medicine, Stanford University. Nuclei were prepared and digested with 1, 3 and 10 U/ml of micrococcal nuclease as described above. Twenty μg samples of the DNA purified

from the treated nuclei were then cut to completion with *Bgl*II, and resolved by electrophoresis through a 1.5% agarose gel. Naked DNA control samples were prepared by digesting purified whole genomic DNA with micrococcal nuclease at 3 U/ml in SPC adjusted to 10 mM $CaCl_2$. Internal molecular weight markers for the *INO1* region were purified from digestions of plasmid DNA with *Bgl*II and other restriction endonucleases cutting in the 5′ upstream DNA. These comprised the 879 bp *Bgl*II–*Sac*I, 651 bp *Bgl*II–*Ssp*I, 441 bp *Bgl*II–*Ssp*I, 295 bp *Bgl*II–*Afl*III and 100 bp *Bgl*II– *Cla*I fragments. Gels were blotted and hybridized with either the 100 bp *Bgl*II–*Cla*I or the 295 bp *Bgl*II–*Afl*III fragments to visualize the micrococcal nuclease digestion fragments produced from the locus.

Acknowledgements

We thank our colleagues for helpful discussions during the course of this work, Stefan Lanker and Curt Wittenberg for providing unpublished strains and plasmids, Fred Cross, Susan Henry, Patricia McGraw and Mary Ann Osley for providing plasmids, and William Ross for expert technical assistance with the flow cytometry. M.S.S. was supported by a fellowship from the Spanish Ministry of Education (Ministerio de Educacion y Ciencia, Becas post-doctorales en el extranjero). This research was supported by National Institutes of Health award GM28920 to M.M.S.

References

Almouzni,G., Clark,D.J., Mechali,M. and Wolffe,A.P. (1990) Chromatin assembly on replicating DNA *in vitro*. *Nucleic Acids Res.*, **18**, 5767–5774.

Ambroziak,J. and Henry,S. (1994) *INO2* and *INO4* gene products, positive regulators of phospholipid biosynthesis in *Saccharomyces cerevisiae*, form a complex that binds to the *INO1* promoter. *J. Biol. Chem.*, **269**, 15344–15349.

Arents,G. and Moudrianakis,E.N. (1993) Topography of the histone octamer surface: repeating structural motifs utilized in the docking of nucleosomal DNA. *Proc. Natl Acad. Sci. USA*, **90**, 10489–10493.

Arents,G., Burlingame,R.W., Wang,B.C., Love,W.E. and Moudrianakis, E.N. (1991) The nucleosomal core histone octamer at 3.1 Å resolution: a tripartite protein assembly and a left-handed superhelix. *Proc. Natl Acad. Sci. USA*, **88**, 10148–10152.

Ashburner,B.P. and Lopes,J.M. (1995) Autoregulated expression of the yeast *INO2* and *INO4* helix–loop–helix activator genes effects cooperative regulation on their target genes. *Mol. Cell. Biol.*, **15**, 1709–1715.

Baer,B.W. and Rhodes,D. (1983) Eukaryotic RNA polymerase II binds to nucleosome cores from transcribed genes. *Nature*, **301**, 482–488.

Butler,A.P. and Olins,D.E. (1982) pH effects on the structure of the inner histones. *Biochim. Biophys. Acta*, **698**, 199–203.

Carlson,M., Osmond,B.C. and Botstein,D. (1981) Mutants of yeast defective in sucrose utilization. *Genetics*, **98**, 25–40.

Chan,D.C. and Piette,L.H. (1982) Effect of tyrosyl modifications on nucleosome reconstitution: a spin-labeling study. *Biochemistry*, **21**, 3028–3035.

Chen,H., Li,B. and Workman,J.L. (1994) A histone-binding protein, nucleoplasmin, stimulates transcription factor binding to nucleosomes and factor-induced nucleosome disassembly. *EMBO J.*, **13**, 380–390.

Clark-Adams,C.D., Norris,D., Osley,M.A., Fassler,J.S. and Winston,F. (1988) Changes in histone gene dosage alter transcription in yeast. *Genes Dev.*, **2**, 150–159.

Cross,F.R. (1990) Cell cycle arrest caused by *CLN* gene deficiency in *Saccharomyces cerevisiae* resembles START-I arrest and is independent of the mating-pheromone signalling pathway. *Mol. Cell. Biol.*, **10**, 6482–6490.

Cross,F.R., Hoek,M., McKinney,J.D. and Tinkelenberg,A.H. (1994) Role of Swi4 in cell cycle regulation of *CLN2* expression. *Mol. Cell. Biol.*, **14**, 4779–4787.

Dean-Johnson,M. and Henry,S.A. (1989) Biosynthesis of inositol in yeast. Primary structure of myo-inositol-1-phosphate synthase (EC 5.5.1.4) and functional analysis of its structural gene, the *INO1* locus. *J. Biol. Chem.*, **264**, 1274–1283.

Di Como,C.J., Chang,H. and Arndt,K.T. (1995) Activation of *CLN1* and *CLN2* G1 cyclin gene expression by *BCK2*. *Mol. Cell. Biol.*, **15**, 1835–1846.

Dilworth,S.M., Black,S.J. and Laskey,R.A. (1987) Two complexes that contain histones are required for nucleosome assembly *in vitro*: role of nucleoplasmin and N1 in *Xenopus* egg extracts. *Cell*, **51**, 1009–1018.

Dirick,L., Moll,T., Auer,H. and Nasmyth,K. (1992) A central role for *SWI6* in modulating cell cycle Start-specific transcription in yeast. *Nature*, **357**, 508–513.

Dirick,L., Bohm,T. and Nasmyth,K. (1995) Roles and regulation of Cln-Cdc28 kinases at the start of the cell cycle of *Saccharomyces cerevisiae*. *EMBO J.*, **14**, 4803–4813.

Durrin,L.K., Mann,R.K., Kayne,P.S. and Grunstein,M. (1991) Yeast histone H4 N-terminal sequence is required for promoter activation *in vivo*. *Cell*, **65**, 1023–1031.

Eickbush,T.H. and Moudrianakis,E.N. (1978) The histone core complex: an octamer assembled by two sets of protein–protein interactions. *Biochemistry*, **17**, 4955–4964.

Fassler,J.S. and Winston,F. (1988) Isolation and analysis of a novel class of suppressor of Ty insertion mutations in *Saccharomyces cerevisiae*. *Genetics*, **118**, 203–212.

Galibert,F. *et al*. (1996) Complete nucleotide sequence of *Saccharomyces cerevisiae* chromosome. *EMBO J.*, **15**, 2031–2049.

Gonzalez,P.J. and Palacian,E. (1989) Interaction of RNA polymerase II with structurally altered nucleosomal particles. Transcription is facilitated by loss of one H2A·H2B dimer. *J. Biol. Chem.*, **264**, 18457–18462.

Gonzalez,P.J., Martinez,C. and Palacian,E. (1987) Interaction with RNA polymerase of nucleosomal cores lacking one H2A·H2B dimer. *J. Biol. Chem.*, **262**, 11280–11283.

Gordon,C.N. and Elliot,S.G. (1977) Fractionation of *Saccharomyces cerevisiae* cell populations by centrifugal elutriation. *J. Bacteriol.*, **129**, 97–100.

Hansen,J.C. and Wolffe,A.P. (1994) A role for histones H2A/H2B in chromatin folding and transcriptional repression. *Proc. Natl Acad. Sci. USA*, **91**, 2339–2343.

Happel,A.M., Swanson,M.S. and Winston,F. (1991) The *SNF2*, *SNF5* and *SNF6* genes are required for Ty transcription in *Saccharomyces cerevisiae*. *Genetics*, **128**, 69–77.

Hartwell,L.H. and Weinert,T.A. (1989) Checkpoints: controls that ensure the order of cell cycle events. *Science*, **246**, 629–634.

Hecht,A., Laroche,T., Strahl-Bolsinger,S., Gasser,S.M. and Grunstein,M. (1995) Histone H3 and H4 N-termini interact with SIR3 and SIR4 proteins: a molecular model for the formation of heterochromatin in yeast. *Cell*, **80**, 583–592.

Hereford,L., Fahrner,K., Woolford,J.,Jr, Rosbash,M. and Kaback,D.B. (1979) Isolation of yeast histone genes H2A and H2B. *Cell*, **18**, 1261–1271.

Hereford,L.M., Osley,M.A., Ludwig,J.R. and McLaughlin,C.S. (1981) Cell-cycle regulation of yeast histone mRNA. *Cell*, **24**, 367–375.

Hirsch,J.P. and Henry,S.A. (1986) Expression of the *Saccharomyces cerevisiae* inositol-1-phosphate synthase (*INO1*) gene is regulated by factors that affect phospholipid synthesis. *Mol. Cell. Biol.*, **6**, 3320–3328.

Hirschhorn,J.N., Brown,S.A., Clark,C.D. and Winston,F. (1992) Evidence that *SNF2/SWI2* and *SNF5* activate transcription in yeast by altering chromatin structure. *Genes Dev.*, **6**, 2288–2298.

Hirschhorn,J.N., Bortvin,A.L., Ricupero-Hovasse,S.L. and Winston,F. (1995) A new class of histone H2A mutations in *Saccharomyces cerevisiae* causes specific transcriptional defects *in vivo*. *Mol. Cell. Biol.*, **15**, 1999–2009.

Jackson,V. (1990) *In vivo* studies on the dynamics of histone–DNA interaction: evidence for nucleosome dissolution during replication and transcription and a low level of dissolution independent of both. *Biochemistry*, **29**, 719–731.

Kayne,P.S., Kim,U.J., Han,M., Mullen,J.R., Yoshizaki,F. and Grunstein,M. (1988) Extremely conserved histone H4 N terminus is dispensable for growth but essential for repressing the silent mating loci in yeast. *Cell*, **55**, 27–39.

Kleinschmidt,A.M. and Martinson,H.G. (1984) Role of histone tyrosines in nucleosome formation and histone–histone interaction. *J. Biol. Chem.*, **259**, 497–503.

Koch,C., Schleiffer,A., Ammerer,G. and Nasmyth,K. (1996) Switching transcription on and off during the yeast cell cycle: Cln/Cdc28 kinases activate bound transcription factor SBF (Swi4/Swi6) at start, whereas Clb/Cdc28 kinases displace it from the promoter in G2. *Genes Dev.*, **10**, 129–141.

Kroll,E.S., Hyland,K.M., Hieter,P. and Li,J.J. (1996) Establishing genetic interactions by a synthetic dosage lethality phenotype. *Genetics*, **143**, 95–102.

Kruger,W., Peterson,C.L., Sil,A., Coburn,C., Arents,G., Moudrianakis, E.N. and Herskowitz,I. (1995) Amino acid substitutions in the structured domains of histones H3 and H4 partially relieve the requirement of the yeast SWI/SNF complex for transcription. *Genes Dev.*, **9**, 2770–2779.

Lew,D.J. and Reed,S.I. (1995) A cell cycle checkpoint monitors cell morphogenesis in budding yeast. *J. Cell Biol.*, **129**, 739–749.

Locklear,L.,Jr, Ridsdale,J.A., Bazett-Jones,D.P. and Davie,J.R. (1990) Ultrastructure of transcriptionally competent chromatin. *Nucleic Acids Res.*, **18**, 7015–7024.

Lopes,J.M., Hirsch,J.P., Chorgo,P.A., Schulze,K.L. and Henry,S.A. (1991) Analysis of sequences in the *INO1* promoter that are involved in its regulation by phospholipid precursors. *Nucleic Acids Res.*, **19**, 1687–1693.

Lycan,D., Mikesell,G., Bunger,M. and Breeden,L. (1994) Differential effects of Cdc68 on cell cycle-regulated promoters in *Saccharomyces cerevisiae*. *Mol. Cell. Biol.*, **14**, 7455–7465.

Ma,X., Lu,Q. and Grunstein,M. (1996) A search for proteins that interact genetically with histone H3 and H4 amino termini uncovers novel regulators of the Swe1 kinase in *Saccharomyces cerevisiae*. *Genes Dev.*, **10**, 1327–1340.

Malone,E.A., Clark,C.D., Chiang,A. and Winston,F. (1991) Mutations in *SPT16/CDC68* suppress *cis*- and *trans*-acting mutations that affect promoter function in *Saccharomyces cerevisiae*. *Mol. Cell. Biol.*, **11**, 5710–5717.

Mann,R.K. and Grunstein,M. (1992) Histone H3 N-terminal mutations allow hyperactivation of the yeast *GAL1* gene *in vivo*. *EMBO J.*, **11**, 3297–3306.

Meeks-Wagner,D. and Hartwell,L.H. (1986) Normal stoichiometry of histone dimer sets is necessary for high fidelity of mitotic chromosome transmission. *Cell*, **44**, 43–52.

Megee,P.C., Morgan,B.A., Mittman,B.A. and Smith,M.M. (1990) Genetic analysis of histone H4: essential role of lysines subject to reversible acetylation. *Science*, **247**, 841–845.

Michalski-Scrive,C., Aubert,J.P., Couppez,M., Biserte,G. and Loucheux-Lefebvre,M.H. (1982) UV differential study of the histones H2A–H2B–H3–H4 octamer. *Biochimie*, **64**, 347–355.

Nasmyth,K. and Dirick,L. (1991) The role of *SWI4* and *SWI6* in the activity of G1 cyclins in yeast. *Cell*, **66**, 995–1013.

Nelson,R.G. and Fangman,W.L. (1979) Nucleosome organization of the yeast 2-μ DNA plasmid: a eukaryotic minichromosome. *Proc. Natl Acad. Sci. USA*, **76**, 6515–6519.

Nikoloff,D.M. and Henry,S.A. (1994) Functional characterization of the *INO2* gene of *Saccharomyces cerevisiae*. A positive regulator of phospholipid biosynthesis. *J. Biol. Chem.*, **269**, 7402–7411.

Norris,D. and Osley,M.A. (1987) The two gene pairs encoding H2A and H2B play different roles in the *Saccharomyces cerevisiae* life cycle. *Mol. Cell. Biol.*, **7**, 3473–3481.

Norris,D., Dunn,B. and Osley,M.A. (1988) The effect of histone gene deletions on chromatin structure in *Saccharomyces cerevisiae*. *Science*, **242**, 759–761.

Ogas,J., Andrews,B.J. and Herskowitz,I. (1991) Transcriptional activation of *CLN1*, *CLN2* and a putative new G1 cyclin (*HCS26*) by *SWI4*, a positive regulator of G1-specific transcription. *Cell*, **66**, 1015–1026.

Peterson,C.L. and Tamkun,J.W. (1995) The SWI–SNF complex: a chromatin remodeling machine? *Trends Biochem. Sci.*, **20**, 143–146.

Peterson,C.L., Kruger,W. and Herskowitz,I. (1991) A functional interaction between the C-terminal domain of RNA polymerase II and the negative regulator *SIN1*. *Cell*, **64**, 1135–1143.

Richardson,H.E., Wittenberg,C., Cross,F. and Reed,S.I. (1989) An essential G1 function for cyclin-like proteins in yeast. *Cell*, **59**, 1127–1133.

Rogers,S., Wells,R. and Rechsteiner,M. (1986) Amino acid sequences common to rapidly degraded proteins: the PEST hypothesis. *Science*, **234**, 364–368.

Rose,M.D., Winston,F. and Hieter,P. (1990) *Methods in Yeast Genetics: A Laboratory Course Manual*. Cold Spring Harbor Laboratory Press, Cold Spring Harbor, NY.

Rowley,A., Singer,R.A. and Johnston,G.C. (1991) *CDC68*, a yeast gene that affects regulation of cell proliferation and transcription, encodes a protein with a highly acidic carboxyl terminus. *Mol. Cell. Biol.*, **11**, 5718–5726.

Shortle,D., Novick,P. and Botstein,D. (1984) Construction and genetic characterization of temperature-sensitive mutant alleles of the yeast actin gene. *Proc. Natl Acad. Sci. USA*, **81**, 4889–4893.

Simchen,G., Winston,F., Styles,C.A. and Fink,G.R. (1984) Ty-mediated gene expression of the *LYS2* and *HIS4* genes of *Saccharomyces cerevisiae* is controlled by the same *SPT* genes. *Proc. Natl Acad. Sci. USA*, **81**, 2431–2434.

Smith,M.M. (1991) Mutations that affect chromosomal proteins in yeast. *Methods Cell Biol.*, **35**, 485–523.

Smith,M.M. and Stirling,V.B. (1988) Histone H3 and H4 gene deletions in *Saccharomyces cerevisiae*. *J. Cell Biol.*, **106**, 557–566.

Smith,P.A., Jackson,V. and Chalkley,R. (1984) Two-stage maturation process for newly replicated chromatin. *Biochemistry*, **23**, 1576–1581.

Stuart,D. and Wittenberg,C. (1994) Cell cycle-dependent transcription of *CLN2* is conferred by multiple distinct *cis*-acting regulatory elements. *Mol. Cell. Biol.*, **14**, 4788–4801.

Stuart,D. and Wittenberg,C. (1995) *CLN3*, not positive feedback, determines the timing of *CLN2* transcription in cycling cells. *Genes Dev.*, **9**, 2780–2794.

Swift,S. and McGraw,P. (1995) *INO1-100*: an allele of the *Saccharomyces cerevisiae INO1* gene that is transcribed without the action of the positive factors encoded by the *INO2*, *INO4*, *SWI1*, *SWI2* and *SWI3* genes. *Nucleic Acids Res.*, **23**, 1426–1433.

Taba,M.R., Muroff,I., Lydall,D., Tebb,G. and Nasmyth,K. (1991) Changes in a SWI4,6–DNA-binding complex occur at the time of *HO* gene activation in yeast. *Genes Dev.*, **5**, 2000–2013.

Tyers,M., Tokiwa,G. and Futcher,B. (1993) Comparison of the *Saccharomyces cerevisiae* G1 cyclins: Cln3 may be an upstream activator of Cln1, Cln2 and other cyclins. *EMBO J.*, **12**, 1955–1968.

Weinert,T.A., Kiser,G.L. and Hartwell,L.H. (1994) Mitotic checkpoint genes in budding yeast and the dependence of mitosis on DNA replication and repair. *Genes Dev.*, **8**, 652–665.

Winston,F. and Carlson,M. (1992) Yeast SNF/SWI transcriptional activators and the SPT/SIN chromatin connection. *Trends Genet.*, **8**, 387–391.

Winston,F., Chaleff,D.T., Valent,B. and Fink,G.R. (1984) Mutations affecting Ty-mediated expression of the *HIS4* gene of *Saccharomyces cerevisiae*. *Genetics*, **107**, 179–197.

Wittenberg,C., Sugimoto,K. and Reed,S.I. (1990) G1-specific cyclins of *S.cerevisiae*: cell cycle periodicity, regulation by mating pheromone and association with the p34CDC28 protein kinase. *Cell*, **62**, 225–237.

Worcel,A., Han,S. and Wong,M.L. (1978) Assembly of newly replicated chromatin. *Cell*, **15**, 969–977.

Xu,Q., Johnston,G.C. and Singer,R.A. (1993) The *Saccharomyces cerevisiae* Cdc68 transcription activator is antagonized by San1, a protein implicated in transcriptional silencing. *Mol. Cell. Biol.*, **13**, 7553–7565.

Zweidler,A. (1992) Role of individual histone tyrosines in the formation of the nucleosome complex. *Biochemistry*, **31**, 9205–9211.

Received on August 12, 1996; revised on January 6, 1997